

Atmospheric Monitoring for the Telescope Array

Yamamoto TOKONATSU^{1,*}, Chikawa MICHYUKI², Hayashida NAOAKI¹, Kawakami SABUROU⁴,
Minagawa TAKAHIRO¹, Morizane YUICHIRO², Sasano MASAHIKO³, Theshima MASAHIRO¹,
Yasui KENJI², and The Telescope Array collaboration

¹*Institute for Cosmic Ray Research, University of Tokyo, Tokyo, Japan*

²*Department of Physics, Kinki University, Higashi-Osaka, Japan*

³*Communication Research Laboratory, Tokyo, Japan*

⁴*Department of Physics, Osaka City University, Osaka, Japan*

(Received July 25, 2001)

For the air fluorescence experiments, like the Telescope Array and the HiRes, we use the atmosphere as a part of detector. Atmosphere can be considered as a part of detector. In order to estimate the primary energy of cosmic ray, the measurement of the light transmittance in the atmosphere is essential point. For this reason, the atmospheric monitoring system is one of the most important calibration equipments in these experiments. We will report the current status of the development of the atmospheric monitoring system. Based on the observational results, we will discuss atmospheric monitoring methods.

KEYWORDS: Cosmic Ray, Fluorescence Technique, Atmospheric Monitoring

§1. Introduction

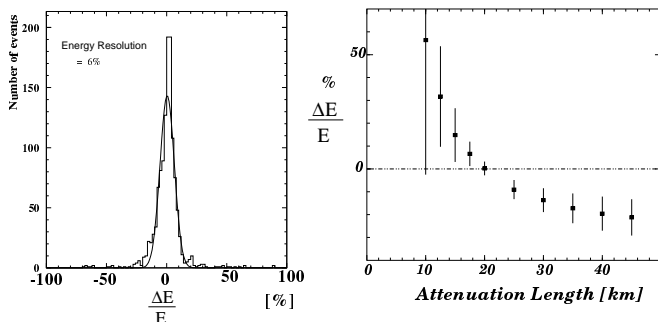


Fig. 1. Results of Monte-Carlo simulation for the Telescope Array. Left panel indicate energy resolution of the Telescope Array for 10^{20} eV cosmic rays. The energy resolution is better than 6% in 1σ as long as we know transmittance of the atmosphere. Right panel shows error of estimated energy for 10^{20} eV cosmic rays as a function of incorrectness of atmospheric correction of attenuation length. The values used for the simulation were $L_M = 20\text{km}$ and $H_M = 1.2\text{km}$.

The air fluorescence technique for air shower observation has many advantages, (for example, direct measurement of shower longitudinal development, stereo geometrical reconstruction with multiple eyes). These aspects will bring technical breakthroughs in EHE Cosmic Ray physics.

On the other hand, this fluorescence technique has a serious problem. In this technique we measure the light yielded from air showers after the transmission in atmosphere of $10 \sim 60$ km distance. Atmosphere can be considered as a part of detector. Without any monitoring,

the atmospheric condition may bring large uncertainty in the experiment and causes the serious systematic error. Therefore, the calibration of the light transmittance in the atmosphere is essential for the air fluorescence experiment.

Charged particles in the air shower excite molecules of the air and yield fluorescence light between 330nm and 400nm. This fluorescence light is also scattered by molecules and aerosols in the air before it reach to the detector. The process by molecules is called as Rayleigh scattering. The attenuation length of this scattering process X_r is 2974 g/cm^2 for 400nm wave length. Then amount of scattered photons with wave length of λ can be calculated by following equation.

$$\frac{dN_r}{dl} = -\rho \frac{N_r}{X_r} \left(\frac{400\text{nm}}{\lambda} \right)^4 \quad (1.1)$$

Where ρ is atmospheric density. In this equation, the number of scattered photons is proportional to λ^{-4} . This scattering process make a serious effect to the observation of fluorescence light in the air.

For example, when we consider the typical measurement of the fluorescence light from an air shower at a distance of 30 km from detector, with the detector altitude of 1.5km and the elevation angle of 30 degrees, the fluorescence light have to pass through about 2200 g/cm^2 in the air and 70% of photons will be scattered by this Rayleigh process.

There is another scattering process, Mie scattering. There are many kinds of scattering matters in the atmosphere, such as, water vapors, mists, clouds, dusts, blown up small sands, artificial fumes, exhaust gas from cars and smokes from forest fires. Furthermore, Kosa from China Gobi desert spread over wide area of northern hemisphere. These atmospheric aerosol's densities and their components change significantly with the location

* E-mail: tokonatu@icrr.u-tokyo.ac.jp

and with the time. The scattering process of photons by these aerosols are called as Mie Scattering. In Utah desert, the typical scale height of Mie scattering H_M is 1.2 km and horizontal attenuation length L_M is 20 km. An amount of scattering photons can be expressed by the following equation.

$$\frac{dN_r}{dl} = -\frac{N_r}{L_M} \times \exp\left(-\frac{h}{H_M}\right) \quad (1.2)$$

Therefore, about 27% photons of air fluorescence light from the air shower are scattered by Mie process with previously mentioned condition. When we take into account the Rayleigh and Mie scattering, about 22% of the photons can reach to our detector.

The Telescope Array (TA) will observe the air showers which flash at far from detector, for example, more than 50km. Fig.1 shows results of Monte-Carlo simulation for TA. According to this simulation study, the energy resolution of TA is better than 6% as far as we know atmospheric transmittance correctly. However, if we apply the 20% shifted value in the attenuation length, the estimated cosmic ray energy have systematic error of nearly 10%. To estimate the primary composition, TA will use X_{max} which is the maximum position in the longitudinal shower development. The intrinsic resolution of X_{max} is estimated to be 20g in TA experiment by the Monte Carlo simulation. If the assumed attenuation length is different by 20%, we estimate X_{max} with 10g systematic error. The correction of atmospheric transmittance affects not only energy determination but also air shower reconstruction. To realize this high resolution power of TA, we need to measure the attenuation length of the atmosphere with an accuracy of a few percent or better.

For the purpose of the atmospheric monitoring, TA and High Resolution Fly's Eyes are developing various methods which use laser or flasher¹⁾²⁾³⁾⁴⁾⁵⁾. One of the well known technique for the atmospheric monitor is LIDAR which is developed for environmental science. Atmospheric conditions can be monitored remotely by measuring back scattered light from a pulsed laser beam in this technique.

We are developing a steerable LIDAR system to study the atmospheric monitoring method in Akeno Observatory. In this paper, we will report details of this system and discuss how to measure the transmittance in the atmosphere accurately.

§2. LIDAR equation

In general, the intensity of the back scattered light detected by LIDAR is expressed by the following equation (LIDAR equation).

$$P(R) = \frac{P_0 \kappa A (c\tau/2) \beta(R) T^2(R) Y(R)}{R^2} + P_b \quad (2.1)$$

$P(R)$: intensity of the detected light

P_0 : laser intensity

P_b : intensity of back ground photons

c : light velocity

R : distance from laser to target

τ : integration time

$Y(R)$: geometrical efficiency of the beam track and receiver

A : aperture of receiver

κ : detector efficiency

β : back scatter coefficient

$T(R)$: transmittance ($=\exp(-\int_0^R \alpha dr)$)

α : extinction coefficient ($=1/\text{attenuation length}$)

We define the following parameters for convenience.

$$P_0 \kappa A \frac{c\tau}{2} Y(R) \equiv C \quad (2.2)$$

$$X(R) \equiv R^2 (P(R) - P_b) \quad (2.3)$$

$$S(R) \equiv \ln(X(R)) \quad (2.4)$$

The LIDAR equation can be then written as follows.

$$X(R) = C \beta(R) T^2(R) = C \beta(R) \cdot \exp(-2 \int_0^R \alpha dr) \quad (2.5)$$

if α is constant until R ,

$$X(R) = C \beta \exp(-2R\alpha) \quad (2.6)$$

Then we obtain differential LIDAR equation.

$$\frac{dS(R)}{dR} = \frac{1}{\beta(R)} \frac{d\beta(R)}{dR} - 2\alpha(R) \quad (2.7)$$

There are two variable parameters in this LIDAR equation. One is the extinction coefficient α that represents the amount of scattered photons in a scattering volume. This value corresponds to the reciprocal of attenuation length. The other variable parameters is back scattering coefficient β that represents the amount of scattered photons in the backward. This value is proportion in density of scattering matter and its differential cross section. Since LIDAR equation has two variables, it can not be solved in general.

If atmosphere is uniform, β is constant and $d\beta/dR = 0$. Then

$$\alpha = -\frac{1}{2} \frac{dS}{dR} \quad (2.8)$$

So we can measure the α using this equation.

If we assume a relationship between α and β , the variable parameters can be reduced. In this purpose, empirical relationship is proposed as follow.

$$\beta = \text{const} \cdot \alpha^k \quad (2.9)$$

In this assumption, k depends on the atmospheric condition and wave length of laser. It is empirically estimated to be 0.6~1.0. Substituting this relationship into equation(2.7), we obtain

$$\frac{dS}{dR} = \frac{k}{\alpha} \frac{d\alpha}{dR} - 2\alpha \quad (2.10)$$

This is Bernoulli type equation.

Viezee adopted the boundary condition near the detector and obtained following solution.⁶⁾

$$\alpha(R) = \frac{X(R)^{1/k}}{\frac{X(R_c)^{1/k}}{\alpha(R_c)} - \frac{2}{k} \int_{R_c}^R X^{1/k}(r) dr} \quad (2.11)$$

Since the second term of the denominator is negative, the denominator approach to the zero with an increase of R . This solution often diverge, and unstable.

Klett proposed a stable solution.⁷⁾ He adopted the boundary condition at farthest point R_c and obtained following solution.

$$\alpha(R) = \frac{X(R)^{1/k}}{\frac{X(R_c)^{1/k}}{\alpha(R_c)} + \frac{2}{k} \int_R^{R_c} X^{1/k}(r) dr} \quad (2.12)$$

In this solution, the integral term of denominator becomes larger with R . Then the contribution of uncertainty of the critical value $\alpha(R_c)$ becomes smaller. Therefore this solution converges on correct value. Using this Klett's method, we can analyze α , if we can assign certain values to the parameter ' k ' and the critical value $\alpha(R_c)$.

Furthermore, Fernald proposed similar solution which consider atmospheric composition.⁸⁾ This solution assume that $k = 1$ and scattering parameter $S_a \equiv \alpha_M/\beta_M$ is constant. Then α can be analyzed in successive steps as the method of Klett. After the invention of these methods, analysis of the LIDAR signal based on the elastic scattering made rapid progress.

§3. Experiment

Wave length[nm]	1064	532	355	266
Pulse Width[nsec]	6-8	5-7	4-6	4-6
Energy [mJ]	50	25	7	5
Pulse Repetition Rage [Hz]	10	10	10	10
Beam Diameter [mm]	2.75	2.5	2	2
Beam Divergence [mrad]	3	3	2	2

Table I. Specification of laser. The type of this laser is Flash lamp pumped, Q-switched and water cooled Nd:YAG laser. We use 355 nm in wave length for this experiment.

The steerable LIDAR system is developed at Akeno Observatory in Yamanashi Prefecture, Japan, its geographical coordinate is 900m a.s.l., 138.5°N, 35.78°E. In this observatory, there are many cosmic ray detectors including the AGASA and fluorescence detectors. Using these detectors, hybrid observation of cosmic rays are going on.

This LIDAR system is constructed on the roof of the Akeno Main laboratory. All of the devices are housed in the astronomical dome that is shown at Fig.2 This astronomical dome consists of a cubic shape room of 1.8mW×1.8mD×1.0mH and a steerable dome. The dome window is opened by 1m, and its direction must be rotated according to the movement of the laser direction. Two motors are equipped for open and close motion and for dome rotation. Each motor is controlled by the electronic switch which operate by the local computer.

The steerable LIDAR system is illustrated in Fig.3. Inside the dome, a laser and optical devices are installed on the optical table which is fixed on the concrete pad.

Prototype of LIDAR System in Akeno

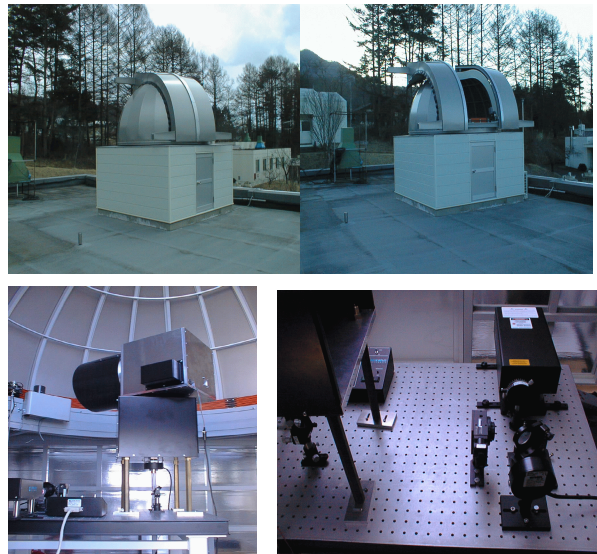


Fig. 2. Akeno Steerable LIDAR System

This laser is flash lamp pumped, Q-switched and water cooled type of Nd:YAG laser. The specification is shown in the table3. The third harmonic beam with wavelength of 355nm is used in this experiment. That wavelength is close to major lines of air fluorescence light. The maximum beam intensity is 7 mJ and maximum repetition rate is 10 Hz. The beam intensity, repetition rate and shooting duration can be controlled by the computer through RS232C.

The laser beam is divided into two directions after phase conversion by the circular polarizer. One is 10% intensity which is used for energy calibration, and the other 90% beam is transported to the shooting system. To stabilize the laser and to prevent from condensation, these optical devices including the laser and the optical table are isolated from atmosphere outside by a fireproof curtain and kept temperature constant by an air conditioner.

An alt-azimuth mount are adopted for the shooting system. Encoders are mounted on the each axis directly. The resolution of these encoders is 5/1000 degree. Each axis is driven by AC stepping motors with 0.0072 degree step. The maximum speed of this shooting system is more than 10 degrees/sec.

An infrared camera is also mounted on the azimuthal axis. Using this infrared camera, cloud can be recognized as the hot region in the cool night sky. The typical temperature of cloud is higher than few degrees, however the typical night sky temperature is lower than -10

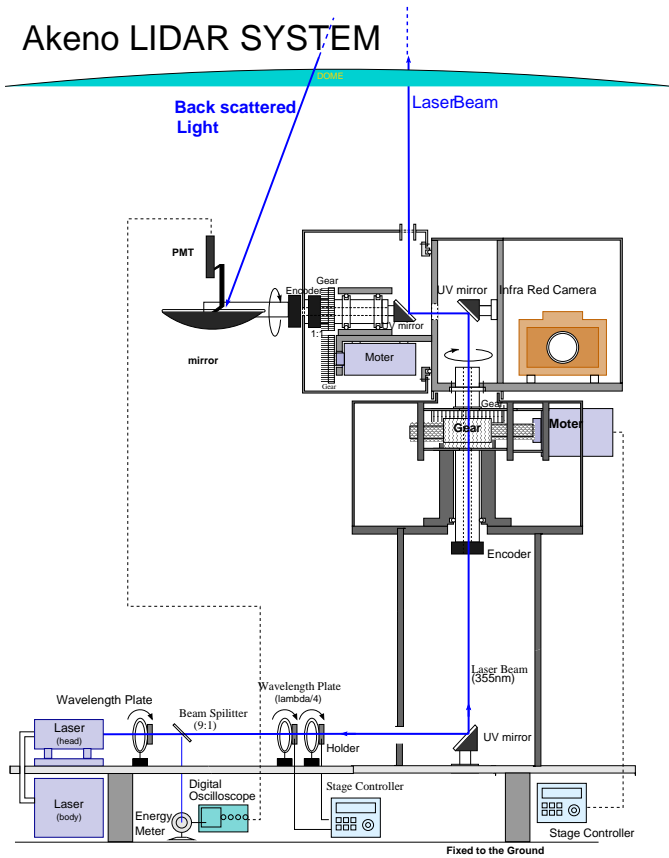


Fig. 3. Diagram of the steerable LIDAR system developed at Akeno observatory.

degrees. This infrared camera can measure the temperature between -20 and 20 degrees and its field of view is 20×40 degrees. To increase data rate, the video image from this camera is captured as ppm format image file through VIDEO capture board.

On the elevation axis, two mirrors are mounted. One is shooting mirror for laser beam. The other is receiving mirror for back scattered light. Maximum beam intensity shot to the sky is about 5 mJ. The receiving mirror adjusted to parallel with the laser beam. Parabolic mirror with 16 cm diameter is adopted for this receiving system. Because the shooting and receiving mirror are mounted on the same part, laser beam and receiver can be moved together. One inch PMT is located at the focus of 16 cm diameter mirror. The field of view is about 1 degree. PMT gain is adjusted to about 10^6 . The signal from PMT is acquired by 100 MHz band width Digital Oscilloscope (TDS33014 made by Tektronix cooperation) which measure the time profile of the back scattered light. The time range of the signal sweep is set to $10 \mu\text{sec}/\text{DIV}$ and the one sweep consists of 500 words with time resolution of 200 nsec. Since the timing of the backscattered light in LIDAR system corresponds to the round-trip time to the target, 200 nsec time resolution is equivalent to 30 m in spatial resolution ΔR . When we set 1 bit to 0.4 mV (it correspond to 10 mV/DIV with 256 bits digitizer), then 1 bit correspond to about 2 photo-electrons. Average of 16 shots is calculated by this oscilloscope and recorded

on the local computer.

All of these systems are controlled by the local computer with Linux operating system and operated by the remote computer through network.

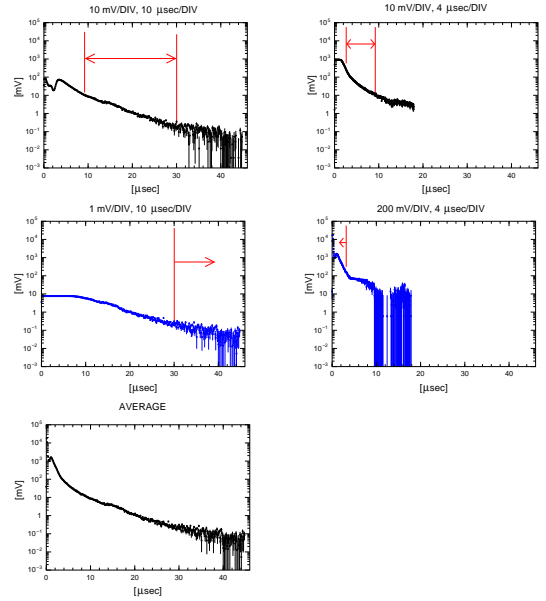


Fig. 4. Example of a time profile of one direction. Average of 1024 shots in vertical direction are plotted. To increase dynamic range, we use two channels: high sensitivity channels (left panels) and low sensitivity channels (right panels). Laser intensity is 5 mJ for high sensitivity channel and 0.4 mJ for low sensitivity channel. The amplitude of low sensitivity channel is normalized by laser intensity. Each sensitivity channel is measured by two ranges of oscilloscope as indicated on title. The regions which are indicated by red lines are used for the analysis. Lower panel indicate average of the four channels.

§4. Observation

The Telescope Array is planned to build 10 stations with 40 km separation in the desert of Utah, USA. The location of those stations will be spread over very wide area, the operation of them should be done remotely via network with microwave link or optic fiber. This would be a severe constraint of our atmospheric monitoring system. For this reason, we developed fully automated system at Akeno observatory. For example, if it begin to rain during the observation, the system is shut down automatically.

The intensity of the back scattered light reaching to the detector from scattering point is proportional to the inverse of the square of the distance, the density of the atmosphere and the intensity of the laser beam. In this reason, returned light from near the detector is huge and faint from far point. Therefore the very wide dynamic range, typically, 4 orders of magnitudes, is required for the light receiving detector. The LIDAR technique has potentially this severe problem. If we use high intensity laser beam, the PMT is saturated by photons scattered near the detector. If it is weak, the number of measurement have to be increased to measure the signal from distant place, then observation time becomes longer.

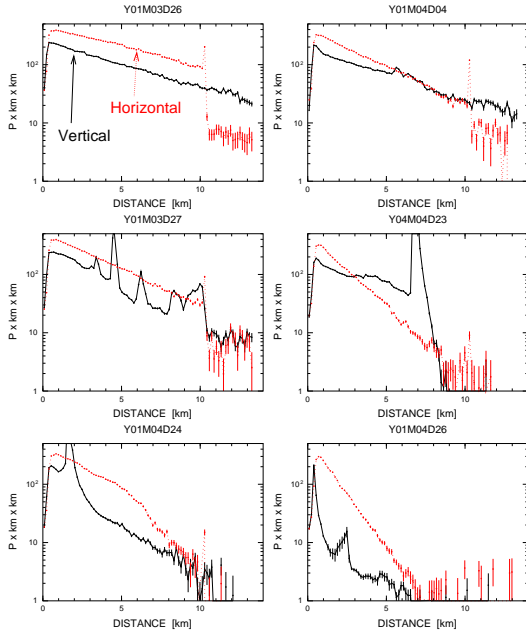


Fig. 5. X-axis is distance from laser. Y-axis is pulse height multiplied by square of distance ($X(R)$). Dotted line indicate the horizontal measurement. Solid line indicate vertical measurement. Upper left panel is result of clear night. Lower right panel is result of cloudy night.

To increase the dynamic range, we use two channels: low and high sensitivity channels. Each channel uses two settings of the digital oscilloscope as illustrated in Fig.4. For high sensitivity channel, laser beam is shot with 5 mJ to the sky and ranges of the oscilloscope are adjusted to 1mV/DIV and 10mV/DIV. In this case, the PMT is saturated by scattered photons near the detector and it take more than 9 μ sec to recover of the sensitivity. Data points with the signal amplitude less than 2 mV are not used in the analysis to obtain reasonable signal to noise ratio, and to reduce the uncertainty of pedestal. This value corresponds to about 1 p.e. i.e. 5 bits for 1mV/DIV. For low sensitivity channel, the laser intensity is reduced to about 1/12 and ranges of the oscilloscope are adjusted to 10mV/DIV and 200mV/DIV. In this case, the PMT recover until 3 μ sec. Using this channel, we can measure the back scattered light from the distance between 1.2 km and 3 km.

The signal profiles of 16 shots are averaged by the digital oscilloscope and then recorded by the local computer. This measurement is repeated 48 times in vertical and horizontal directions and 16 times for every 5 degrees in zenith angle. In other word, 1024 shots are measured in vertical and horizontal directions, and 256 shots are measured in other directions.

Examples of measurements are shown in Fig.5. In this figure, results of vertical and horizontal directions are shown. In the horizontal measurement, if the atmosphere depends on only altitude (it means atmosphere has 1-D structure and is uniform), $S(R) \equiv \log(X(R))$ is in proportion to R and extinction coefficient α is analyzed by the slope using equation(2.8). If atmosphere is not uniform in the horizontal direction, the slope is not

constant, depending on the atmospheric condition. We can see $S(R)$ decline linearly until 10 km under the good weather in Fig.5 There is a mountain at the distance of 10km and the scattered light by this mountain can be seen in this figure. The atmosphere is not uniform under the bad weather and $S(R)$ dose not decline linearly. In the measurement in the vertical direction, it can be seen clearly that the signal strength varies rapidly up and down at the place of cloud. We can measure the atmosphere up to 12 km altitude under the clear sky.

§5. Analysis

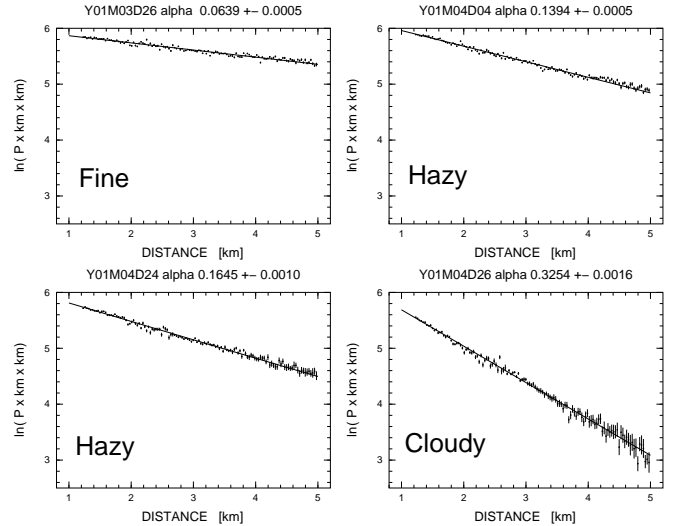


Fig. 6. Example of horizontal measurement. Region from 1.2 km to 5 km are plotted. The upper left panel is clearest night, and lower right panel is cloudy night. Solid line is result of fitting by straight line. The extinction coefficient α can be estimated by the slope of this line. The estimated α is indicated on the title.

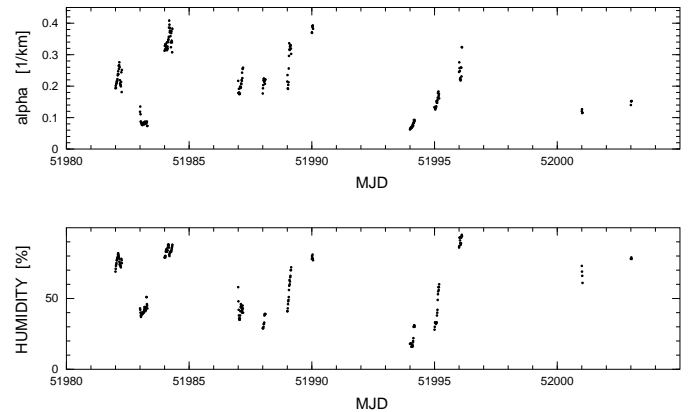


Fig. 7. Upper panel shows estimated α at the level of the detector as a function of observation time. Lower panel shows humidity which measured simultaneously.

In this section, we discuss how to estimate the transmittance of the atmosphere using the results of the measurements described above.

One of the simplest case is horizontal measurement. If

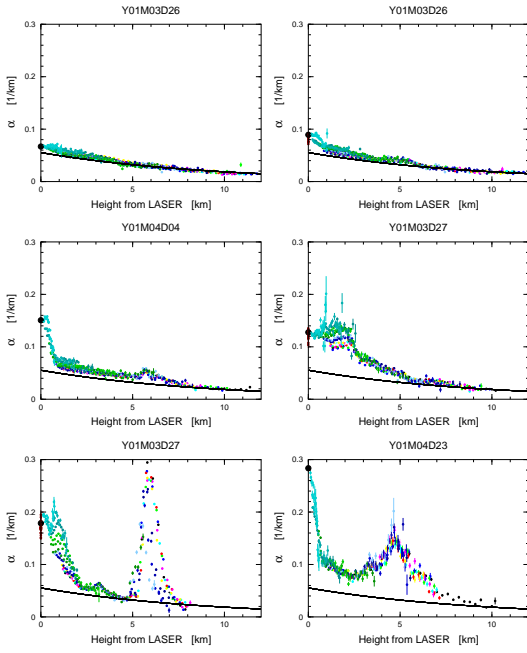


Fig. 8. Estimated α using Klett's method as a function of altitude. Different colors correspond to different zenith angle. Solid line indicates the expected value from Rayleigh scattering. The black dot at height 0 indicates the measured value in horizontal shot. Upper left panel is result of clearest night. In lower left panel, we can see cloud around 6km altitude. This cloud obscures the signal from higher altitude. Because boundary condition can not be determined, the absolute value can not be analyzed correctly.

the atmosphere is uniform, α can be analyzed by equation(2.8) in level of the detector as mentioned before. Fig.6 shows examples of this horizontal measurement. The data which is comparatively near the detector is used. It can be seen that the attenuation of the laser beam depends clearly on the weather. It can also be confirmed that the atmosphere is uniform in this region. Fig.6 shows the time profile of α comparison with humidity which is measured simultaneously. Of course, transmittance of the atmosphere depend on not only humidity, however we can see that variation of α follows the tiny variation of the humidity in this figure. This method appears to be very convincing and accurate.

As described section2, the LIDAR equation can not be solved because it have two variable parameters. A solution which use an assumption of the empirical relationship between α and β is proposed by Klett. To estimate α using Klett's method, we need to determine two parameters: One is the critical value at the highest altitude point. The other is a parameter k which represent of the relationship between α and β . To determine these parameters, we use a simple assumption as follows.

- In the measurement in vertical direction, the smallest α corresponds to the value expected from Rayleigh scattering. If there is no cloud, this value can be estimated at the highest point.
- In the measurement in a different direction, a smaller α (meaning the value in a region of no cloud) corresponds to the α which is measured at a direc-

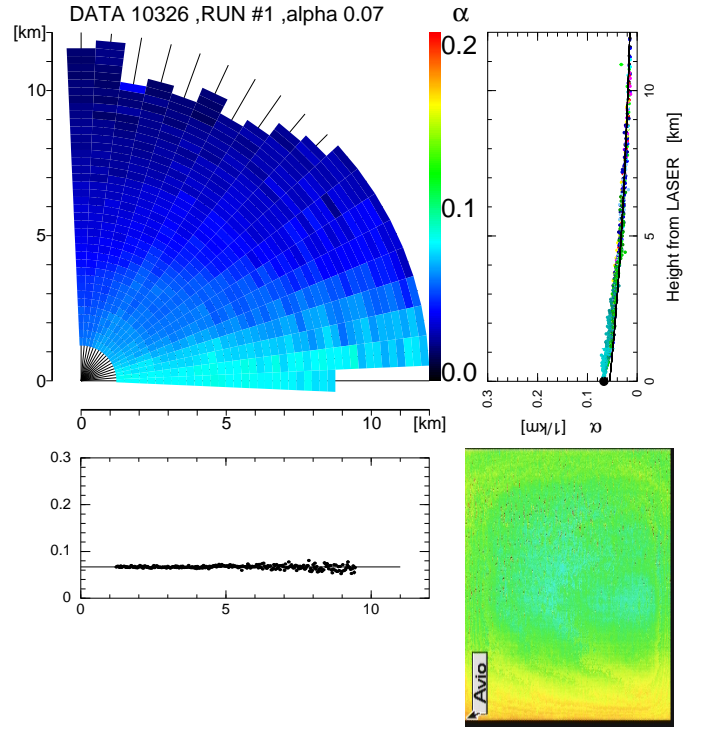


Fig. 9. An example of estimated extinction coefficient α . Upper left panel shows a two dimensional map of α inside a 12 km radius circle from LIDAR. Estimated α in horizontal measurement is indicated in title. Upper right panel is same with previous figure. Lower left panel shows the estimated extinction coefficient in a horizontal shots. The solid line indicates result of fitting. Lower right panel shows an image from infrared camera. It was clearest night.

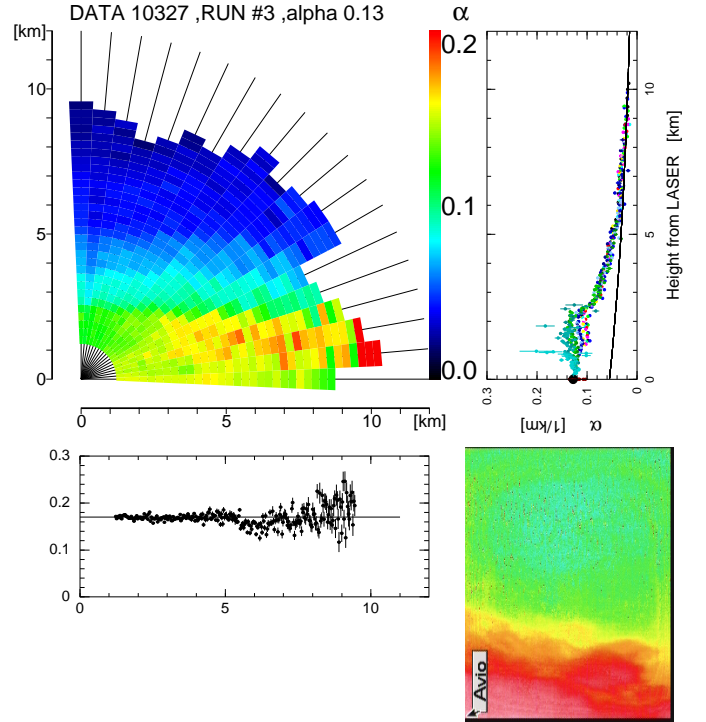


Fig. 10. The next night data. The expression is the same as the previous figure. It was hazy at low altitude.

tion of ± 5 degrees at the same altitude.

- α at points lower than 100m can be estimated by the α obtained in the horizontal measurement.

In the first assumption, it is necessary that the atmosphere is clear and the effect of Mie scattering can be ignored at the high altitude. This assumption is reasonable under the good weather. However if it is bad weather, this assumption causes the most significant systematic error. In the second assumption, it is necessary that the atmosphere depends on only altitude on average. If all of the sky is covered with cloud, it is impossible to estimate the α because of this assumption. In general, the Telescope Array will observe under the clear sky, these assumptions should be acceptable. With these assumptions, we can determine the parameter 'k' and the critical value.

Fig.8 shows the examples of estimated α as a function of altitude at each zenith angle. As we can see, atmosphere is almost uniform if there is no cloud. In lower left panel, we can see cloud around 6 km altitude. This cloud obscures the signal from higher altitude. Since boundary condition at high altitude can not be determined, the absolute value of α can not be analyzed correctly. Fig.9 is the result of a very clear night. It was able to measure distance more than 12 km. The atmosphere of this night can be almost explained by pure molecular at high altitude. Also it was very uniform as is illustrated. It can be clearly seen that statistical error is very small at all points. For example, the transmittance between detector and a 10 km distance in the vertical direction is estimated to be 73.27% with statistical error of 0.05%. Fig.10 shows the result of measurement on the next night. It was hazy and the atmosphere was not uniform at lower heights. The transmittance between detector and 10km distance in the vertical direction is 57.91% with statistical error of 0.07% It takes about 20 minutes measurement in these cases.

§6. Systematic Error

The systematic error in the present analysis based on Klett's method has been investigated using a simple Monte-Carlo simulation.⁹⁾ In this simulation, signal profile of back scattered light was calculated by simple atmospheric model. Number of scattered photons by Rayleigh scattering is calculated by standard desert model and Mie scattering is calculated with Mie parameters, the scale height H_M and attenuation length of horizontal L_M . The effect of multi-scattering is ignored here. An example of atmospheric model with typical Mie parameters is shown in Fig.11. In this figure, elevation angle of laser is assumed to be 10 degrees. This artificial data is analyzed by same programs with real data analysis. Fig.12 shows examples of this simulation. In this figure expected α which is calculated by inputted atmospheric model and estimated one using Klett's method are compared. The inputted and estimated α is slightly different. Especially the effect of Mie scattering can not be ignored at high altitude with large H_M . Therefore estimated value is different from expected one at high altitude. However, if H_M is reasonable value, the dif-

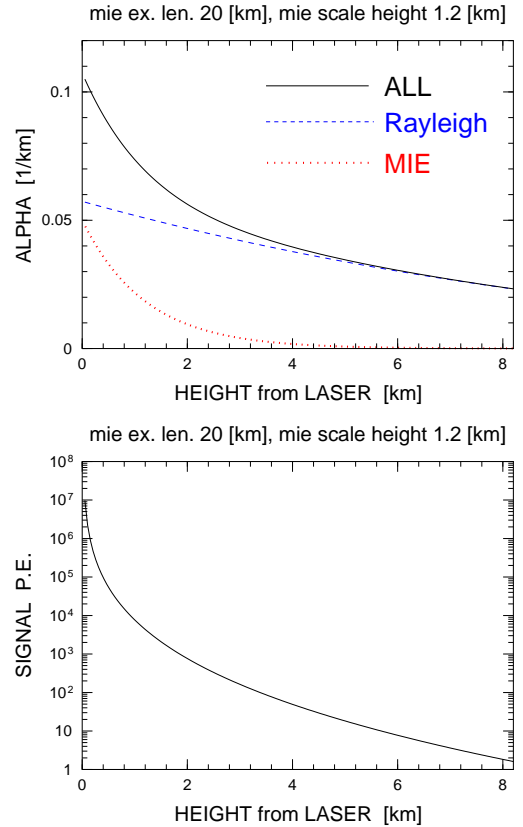


Fig. 11. An example of atmospheric model which is used for simulation. Typical values of Mie parameters are used for this simulation as indicated on title. The diameter of receiver mirror is 1.5m, laser intensity is 10mJ and elevation angle of laser is 10 degrees. In upper panel, dashed and dotted line indicates expected α from Rayleigh and Mie scattering respectively. Solid line indicates expected α from both scattering. Lower panel shows expected number of photo-electrons which detected by LIDAR.

ference can be acceptable. Fig.13 shows the systematic error of attenuation length with various Mie parameters. According this figure, the systematic error which caused by Klett's method is about 0.5% with the typical atmospheric model ($L_M=20\text{km}$, $H_M=1.2\text{km}$).

The detector constants (for example: mirror reflectivity, PMT gain, beam intensity and so no) do not contribute to the systematic errors in this analysis except for the linearity of the PMT. The effect of multiple scattering is ignored in this measurement. The most significant systematic error is caused by the uncertainty in the critical value. The altitude of 10 km, where we gave the boundary condition, may not high enough to ignore the effect of Mie scattering. This problem can be solved if we use larger mirror or higher intensity laser.

§7. Summary

We have developed a steerable LIDAR system for atmospheric monitoring for the Telescope Array. The system consists of a 5 mJ pulse laser and 16 cm diameter mirror. Using this system, a technique for atmospheric monitoring was developed.

Firstly, the extinction coefficient α at the level of the detector is measured. Then α is estimated at all direc-

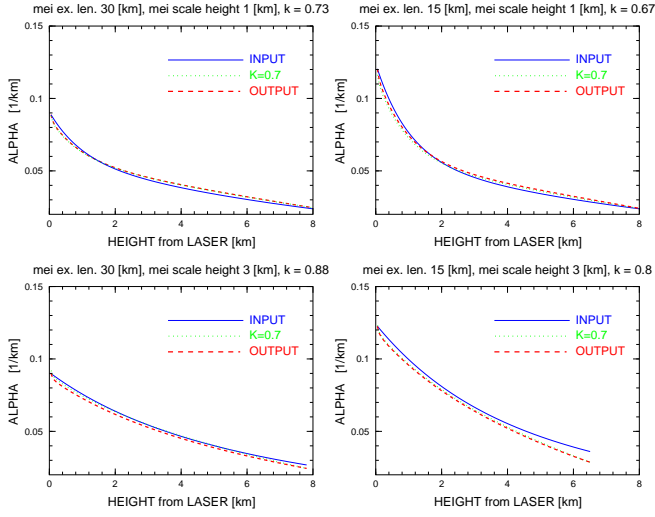


Fig. 12. Examples of result of simulation. Inputted values of Mie parameters are indicated on title. Solid line indicates the true value which is calculated from each atmospheric model. Dotted line indicates estimated α using Klett's method under the assumption of $k = 0.7$. Dashed line indicates estimated α which is assumed we know the α at level of detector. Estimated k is indicated on title.

tions using Klett's method. The transmittance of the night sky to a distance more than 10 km can be measured successfully. The statistical error in this analysis is less than 2% under the clear sky. It takes 20 minutes to measure one azimuthal direction.

The systematic error which is caused by this analysis method is estimated about 0.5% under the typical atmospheric model. The detector constants do not contribute to the systematic errors in this analysis except for the linearity of the PMT. The most significant systematic error is caused by uncertainty in the critical value. This problem can be solved if we use larger mirror or higher intensity laser.

Based on these observational results, we are considering future plans of the atmospheric monitoring for the Telescope Array. Signal to noise ratio is in proportion to beam intensity, mirror diameter, square root of observation time and transmittance. $5mJ \times 16cm \times \sqrt{20min} = 358[mJ \cdot cm \cdot min^{1/2}]$ is required to measure up to the distance of 10km under the clear sky (in this case transmittance is about 60% in vertical direction). To measure more than 50 km, we need $358 \times 5^2 / 0.6^5 = 115000[mJ \cdot cm \cdot min^{1/2}]$. This means a 270 mJ laser is necessary for 3 m diameter mirror if we want to measure one azimuthal direction in 2 minutes. This value will be reduced by narrow band filter, small field of view and high altitude location.

Acknowledgements

This work is supported by grants in aid #12304012 and #11691117 for the scientific research of JSPS(Japan Society for the Promotion of Science). The authors thank Dr. Lawrence R. Wiencke, Dr. Michael E. Roberts and Prof. John A.J.Matthews for creative discussion.

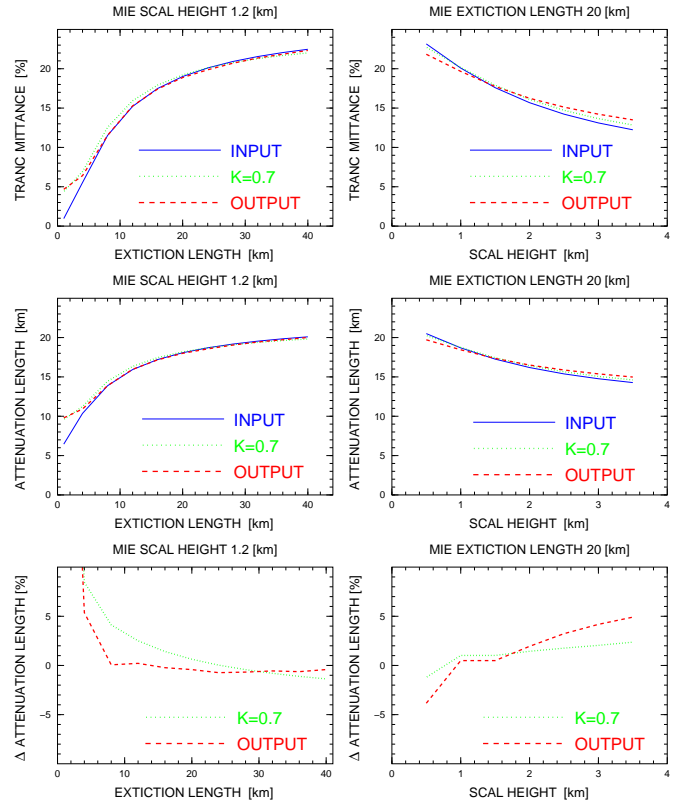


Fig. 13. Estimated systematic error as a function of Mie parameters. In case of left panels, L_M is varied and H_M is fixed to typical value. In case of right panels, H_M is varied and L_M is fixed. Upper and middle panel show the transmittance and the attenuation length between the detector and 30km distance respectively. Lower panels show the estimated systematic error. Solid line indicates the true value. Dotted line indicates the estimated value under the assumption of $k = 0.7$. Dashed line indicates estimated α which is assumed we know the α at level of detector.

- 1) L.R.Wiencke, *et all* : NIM A **428**(1999)593-607
- 2) M.Chikawa, *et all* : Proceedings of the 26th ICRC (1999)OG4.5.17
- 3) R.Gray, *et all* : Proceedings of the 26th ICRC (1999)OG4.5.04
- 4) N.Hayashida, *et all* : Proceedings of the 26th ICRC (1999)OG4.5.05
- 5) J.R.Mumford, *et all* : Proceedings of the 26th ICRC (1999)OG4.5.10
- 6) W.Viezee, J.Oblanas, R.T.H.Collis:SRI report AFCRL-TR-73-0708(1973)
- 7) J.D.Klett : Appl.Optics,**20**(1981)211-220
- 8) F.G.Fernald : Appl.Optics,**23**(1984)652-653
- 9) John A.J.Matthews : private communication(2001)